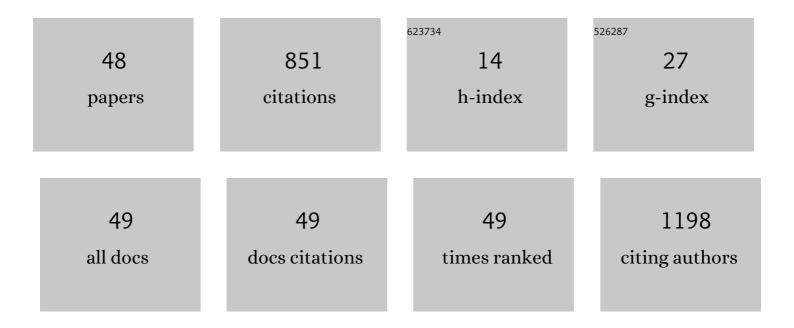
Richard S Smith

List of Publications by Year in descending order

Source: https://exaly.com/author-pdf/8108738/publications.pdf Version: 2024-02-01



RICHARD S SMITH

#	Article	IF	CITATIONS
1	Estimating the parameters of simple models from two-component on-time airborne electromagnetic data. Geophysics, 2022, 87, JM15-JM27.	2.6	0
2	Transformation of magnetic data to the pole and vertical dip and a related apparent susceptibility transform: Exact and approximate approaches. Geophysics, 2022, 87, G1-G14.	2.6	4
3	Multiple-order moments of the transient electromagnetic response of a one-dimensional earth with finite conductance – theory. Exploration Geophysics, 2021, 52, 1-15.	1.1	2
4	RCL1 copy number variants are associated with a range of neuropsychiatric phenotypes. Molecular Psychiatry, 2021, 26, 1706-1718.	7.9	10
5	A recurrent, homozygous EMC10 frameshift variant is associated with a syndrome of developmental delay with variable seizures and dysmorphic features. Genetics in Medicine, 2021, 23, 1158-1162.	2.4	13
6	16p11.2 deletion is associated with hyperactivation of human iPSC-derived dopaminergic neuron networks and is rescued by RHOA inhibition in vitro. Nature Communications, 2021, 12, 2897.	12.8	35
7	Early role for a Na ⁺ ,K ⁺ -ATPase (<i>ATP1A3</i>) in brain development. Proceedings of the National Academy of Sciences of the United States of America, 2021, 118, .	7.1	20
8	Regulation of human cerebral cortical development by EXOC7 and EXOC8, components of the exocyst complex, and roles in neural progenitor cell proliferation and survival. Genetics in Medicine, 2020, 22, 1040-1050.	2.4	13
9	Ion Channel Functions in Early Brain Development. Trends in Neurosciences, 2020, 43, 103-114.	8.6	67
10	A new method for interpolating linear features in aeromagnetic data. Geophysics, 2019, 84, JM15-JM24.	2.6	10
11	Structural complexity inferred from anisotropic resistivity: Example from airborne EM and compilation of historical resistivity/induced polarization data from the gold-rich Canadian Malartic district, Québec, Canada. Geophysics, 2019, 84, B153-B167.	2.6	11
12	Aspm knockout ferret reveals an evolutionary mechanism governing cerebral cortical size. Nature, 2018, 556, 370-375.	27.8	127
13	An airborne electromagnetic system with a three-component transmitter and three-component receiver capable of detecting extremely conductive bodies. Geophysics, 2018, 83, E347-E356.	2.6	3
14	The ESCRT-III Protein CHMP1A Mediates Secretion of Sonic Hedgehog on a Distinctive Subtype of Extracellular Vesicles. Cell Reports, 2018, 24, 973-986.e8.	6.4	79
15	Sodium Channel SCN3A (NaV1.3) Regulation of Human Cerebral Cortical Folding and Oral Motor Development. Neuron, 2018, 99, 905-913.e7.	8.1	109
16	The impact of magnetic viscosity on time-domain electromagnetic data from iron oxide minerals embedded in rocks at Opemiska, Québec, Canada. Geophysics, 2017, 82, B165-B176.	2.6	6
17	Precision requirements for specifying transmitter waveforms used for modelling the off-time electromagnetic response. Exploration Geophysics, 2013, 44, 1-5.	1.1	6
18	Sensitivity cross-sections in airborne electromagnetic methods using discrete conductors. Exploration Geophysics, 2012, 43, 95-103.	1.1	15

RICHARD S SMITH

#	Article	IF	CITATIONS
19	A grid implementation of the SLUTH algorithm for visualising the depth and structural index of magnetic sources. Computers and Geosciences, 2012, 44, 100-108.	4.2	5
20	Qualitative geophysical interpretation of the Sudbury structure. , 2012, , .		0
21	Metalliferous mining geophysics — State of the art after a decade in the new millennium. Geophysics, 2011, 76, W31-W50.	2.6	52
22	A comparison of airborne electromagnetic data with ground resistivity data over the Midwest deposit in the Athabasca basin. Near Surface Geophysics, 2011, 9, 319-330.	1.2	11
23	Case history of combined airborne time-domain electromagnetics and power-line field survey in Chibougamau, Canada. Geophysics, 2010, 75, B67-B72.	2.6	17
24	Detection of alteration at the Millennium uranium deposit in the Athabasca Basin: a comparison of data from two airborne electromagnetic systems with ground resistivity data. Geophysical Prospecting, 2010, 58, 1147-1158.	1.9	6
25	Case histories illustrating the characteristics of the HeliGEOTEM system. Exploration Geophysics, 2009, 40, 246-256.	1.1	16
26	Application of Occam's inversion to airborne time-domain electromagnetics. The Leading Edge, 2009, 28, 284-287.	0.7	31
27	Mapping tailings around mine sites with reverse polarity airborne transient EM data. , 2008, , .		0
28	Geological mapping with power line fields measured with MEGATEM data. , 2008, , .		0
29	A discrete conductor transformation of airborne electromagnetic data. Near Surface Geophysics, 2007, 5, 87-95.	1.2	13
30	Airborne EM measurements over the Shea Creek uranium prospect, Saskatchewan, Canada. , 2006, , .		4
31	Combining airborne electromagnetic data from alternating flight directions to form a virtual symmetric array. Geophysics, 2006, 71, G35-G41.	2.6	10
32	An analysis of geophysical and geological data from the Iso/New Insco test site, Quebec, Canada. , 2006, , .		0
33	Approximate apparent conductance (or conductivity) from the realizable moments of the impulse response. Geophysics, 2005, 70, G29-G32.	2.6	12
34	An enhanced method for source parameter imaging of magnetic data collected for mineral exploration. Geophysical Prospecting, 2005, 53, 655-665.	1.9	16
35	Interpolation and gridding of aliased geophysical data using constrained anisotropic diffusion to enhance trends. Geophysics, 2005, 70, V121-V127.	2.6	25
36	Gridding aeromagnetic data using longitudinal and transverse horizontal gradients with the minimum curvature operator. The Leading Edge, 2005, 24, 142-145.	0.7	25

RICHARD S SMITH

#	Article	IF	CITATIONS
37	Imaging depth, structure, and susceptibility from magnetic data: The advanced source-parameter imaging method. Geophysics, 2005, 70, L31-L38.	2.6	41
38	Interpolation and gridding of aliased geophysical data using constrained anisotropic diffusion to enhance trends. , 2004, , .		0
39	Using realizable moments of the impulse response to estimate the approximate apparent conductance or apparent conductivity of the ground. , 2004, , .		1
40	Combining airborne electromagnetic data from alternate flight directions to improve data interpretability: the virtual symmetric array. , 2004, , .		1
41	Using airborne EM surveys to investigate the hydrogeology of an area near Nyborg, Denmark. , 2004, , .		Ο
42	Using a non-integer moment of the impulse response to estimate the half-space conductivity. Geophysical Prospecting, 2003, 51, 443-446.	1.9	7
43	The moments of the impulse response, a new paradigm for the interpretation of transient electromagnetic data. , 2002, , .		Ο
44	Using the moments of a thick layer to map conductance and conductivity from airborne electromagnetic data. Journal of Applied Geophysics, 2002, 49, 173-183.	2.1	11
45	An experiment to compare airborne, semiâ€airborne and ground electromagnetic systems. , 2000, , .		Ο
46	Modelâ€independent depth estimation with the SPIâ,,¢ method. , 1999, , .		12
47	Geology from geophysics; or, converting magnetic data to depth, dip, and susceptibility contrast using the source parameter imaging (SPITM) method. , 1996, , .		2
48	Multiple-order moments of the transient electromagnetic response of a one-dimensional earth with finite conductance – the Gaussian variation applied to a field example. Exploration Geophysics, 0, , 1-13.	1.1	2